W. G. Reuter, S. M. Graham*, W. R. Lloyd*, and R. L. Williamson**

Ability of Using Experimental Measurements of δ to Predict Crack Initiation for Structural Components

REFERENCE Reuter, W. G., Graham, S. M., Lloyd, W. R., and Williamson, R. L., **Ability of using experimental measurements of δ to predict crack initiation for structural components**, *Defect Assessment in Components – Fundamentals and Applications*, ESIS/EGF9 (Edited by J. G. Blauel and K.-H. Schwalbe) 1991, Mechanical Engineering Publications, London, pp. 175–188.

ABSTRACT Fracture mechanics data are used to predict structural integrity. But, because it is too expensive to test structural components under realistic conditions, the ability to make accurate predictions has not been quantified. This paper compares data from specimens containing surface cracks or centre cracks, which simulate structural components, with data from standard fracture toughness specimens (C(T) or SEN(B) specimens per ASTME 813) to evaluate the accuracy of using standard data to predict initiation of crack growth for the surface cracked specimens in the non-linear elastic fracture mechanics (NLEFM) regime. Hydrostatic stress is used to quantify the constraint of the specimens. This paper identifies a basis for measuring crack tip opening displacement (δ) and identifies specific values of δ (δ_{init} and δ_i) associated with initiation of crack growth in these specimens. These data are used to compare δ_{init} and δ_i as a function of constraint for the three specimen configurations.

Introduction

Fracture mechanics data, obtained from standardized specimens, are used in alloy development, material selection, and material procurement because they are more sensitive than other mechanical properties data to metallurgical changes. Fracture mechanics data are also used to predict crack growth initiation and growth under monotonic loading; this is the subject of our research. The general approach is to measure fracture toughness by appropriate techniques and then use these data to predict failure conditions (initiation of crack growth, penetration of the wall thickness or catastrophic failure) for structural components. There are very few instances, except in failure analyses, where comparisons have been made between predictions and actual results obtained from tests of structural components. This is due to the high cost of testing components under realistic stress/temperature conditions. At the Idaho National Engineering Laboratory (INEL), surface-cracked specimens are being used to simulate the fracture behaviour of structural components. Test results obtained from these specimens are compared with predictions made using data developed from compact tension C(T) or three-point bend SEN(B) specimens and existing models.

Under non-linear elastic fracture mechanics (NLEFM) conditions, the fracture process consists of nucleation of a crack, blunting, initiation of crack growth, subcritical crack growth, and sometimes instability. The process of

* Idaho National Engineering Laboratory, Idaho Falls, Idaho 83415-2218, USA.

nucleation of a crack is ignored in this work as it is assumed that a sharp crack already exists in the structure. This study is concerned with establishing the conditions associated with initiation of growth of an existing crack. These conditions are expected to be mechanical properties of the material. The standard fracture toughness measurement, δ_i, which is associated with initiation of subcritical crack growth, is a critical value of crack tip opening displacement(s) corresponding to 0.20 mm of crack growth, including the stretch zone width (SZW), over the full crack width **(1)**. The SZW is the crack length extension that occurs during crack-tip blunting. For specimens containing surface cracks, crack growth initiation ($\Delta a > 0$) may be any detectable crack front perturbation regardless of the length of crack front over which it occurred. The crack tip opening displacement (δ) associated with crack growth initiation is designated as δ_{init}. Thus a comparison between δ_{init} of the surface crack and δ_i from standard specimens may not be valid since they may not be measurements of the same event. It is necessary to establish a constant event for these comparisons. Because δ can be measured experimentally from both standard fracture toughness specimens and specimens containing surface flaws, it was used, initially, as the experimental tool for comparison.

The use of a single parameter such as δ is expected to be successful for a two-dimensional crack as long as the specimens experience similar constraint. Values of δ obtained from square section single edge notch bend [SEN(B)] specimens may differ from those measured from C(T) or rectangular SEN(B) specimens **(1)**. This observation is understandable – the square section SEN(B) specimen may have a lower constraint than the C(T) and rectangular SEN(B) specimens which are designed to maximise constraint. Matsoukas *et al.* **(2)** investigated δ for initiation of ductile tearing for shallow and deep cracks and observed that δ was larger for the shallow than for deep cracks. They also showed that the hydrostatic stresses are larger for the deep crack. These results of Matsoukas *et al.* **(2)** suggest that a constraint term is also required when comparing δ for different specimen configurations. Thus, for structures containing the three-dimensional surface crack, it is probable that a constraint parameter will be required in addition to δ determined from laboratory test specimens. Therefore, this paper also evaluates the efficacy of using constraint as the second parameter for predicting crack growth initiation of a structural component using data generated by standard fracture toughness specimens.

It is expected that different values of constraint will be encountered with the standard specimen (SEN(B) and C(T)) and the surface cracked SC specimens. This will provide a basis for evaluating the effectiveness of using constraint as a parameter for comparing δ_{init} values. But, there will be no way to estimate the relationship between these two points. Therefore, a third specimen configuration was used to provide a basis for estimating the relationship between δ_{init} and constraint. A centre-cracked panel CCP specimen tested by tensile loading was chosen since it had the same thickness as the surface-cracked specimens and it reflects a type of defect that may be found in structures.

Materials and test procedures

Specimens were fabricated from as-rolled ASTM A710 Grade A steel plate. The significant mechanical and physical properties of this material, at 297 K, and material chemistry are tabulated below.

Yield strength		*Ultimate tensile strength*				*Young's modulus*		*Poisson's ratio*		
470 *MPa*		636 *MPa*				208.4 *GPa*		*0.236*		
C	*Mn*	*P*	*S*	*Si*	*Cr*	*Ni*	*Mo*	*Cu*	*Cb*	*Fe*
0.05	0.47	0.010	0.004	0.25	0.74	0.85	0.21	1.20	0.038	bal.

Standard C(T) fracture toughness specimen 12.7 mm thick and SEN(B) specimens 15.9 mm thick were tested per ASTM E813 **(3)**. Standard centre cracked tensile CCP specimens were 6.4 mm thick by 101 mm wide with crack length (2a) = 6.4, 13, or 26 mm long. Surface-cracked SC specimens were 6.4 mm thick by 101 mm wide with crack depth (a) = 3.8 mm and crack length (2c) = 25 mm. All of the specimens were fatigue precracked prior to testing. All tests were conducted by monotonically loading to the desired load and then unloading.

The procedure described in ASTM E1290-89 **(1)** for estimating plastic δ_i for SEN(B) and C(T) specimens based on measuring crack growth (Δa) and the plastic component of crack opening displacement was not used because similar procedures are not available for CCP and SC specimens (unless microtopographic techniques are used for all of the specimens). For the conventional test specimens in that procedure, δ_i is at a constant offset value of $\Delta a = 0.2$ mm, which may provide a close estimate of δ_{init} since SZW = $\delta/2$. For the CCP and SC specimens, it is expected that SZW $\neq \delta/2$ since the initial crack tip opening angle (CTOA) is less than 90 degrees. Therefore, for consistency, the following two methods were used to measure Δa and δ.

Slicing technique

Specimens were loaded monotonically to the desired value, unloaded, and made ready for metallographic examination. The slices were taken perpendicular to the plane of the fatigue crack and perpendicular to the face designated as A in Fig. 1. In this procedure the SZW is not included in the measurement of Δa.

Microtopography

Specimens were loaded monotonically to the desired value, unloaded, cooled in liquid nitrogen (LN_2), and loaded to fracture by cleavage. Variations in height, relative to a common plane such as the fatigue crack, were measured as a function of distance along a specified line on each half of a broken specimen.

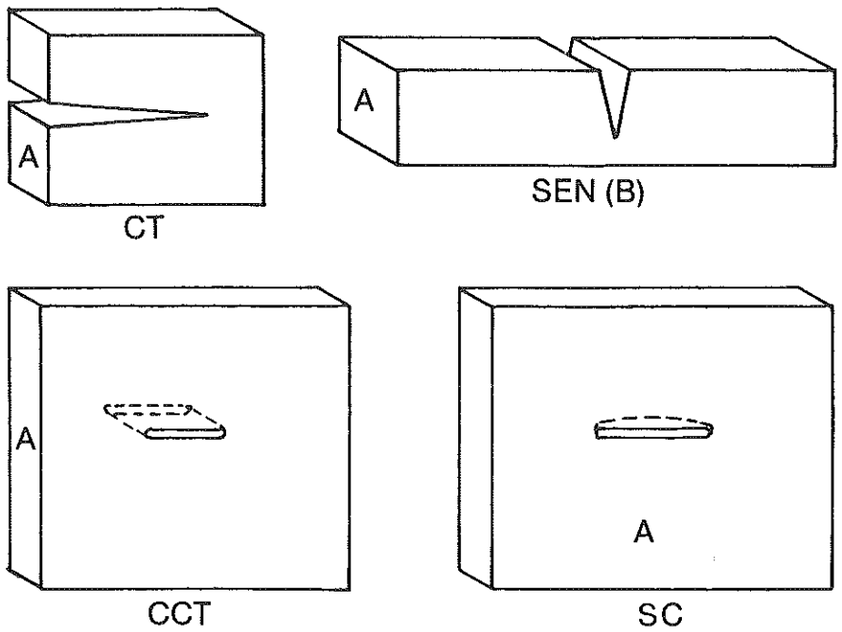

Fig 1 Schematic of test specimens

These lines are perpendicular to the crack front and are at the same location on each half. These data are combined to provide a profile of the crack tip region; therefore, δ and Δa can be measured. Obtaining an accurate reproduction, such as that visible in Fig. 3, of the crack tip region, requires numerous measurements, which were not made because of the cost. The SZW is included in this measurement of Δa in the same manner as in ASTM E1290. Detailed explanations of this method are provided by Kobayashi *et al.* **(4)** and Zhang *et al.* **(5)**.

Typical test results

In all instances, crack initiation preceded attainment of maximum load. The results of the slicing and microtopographic techniques used to measure Δa and δ, are presented below:

Crack growth, Δa

Figure 2 shows representative photographs of the crack tip region for a standard fracture toughness specimen. These photos were taken from slices 1.27 mm apart and it is apparent, from the local fine cracks and other perturbations visible at the tip, that crack growth had occurred and that it is relatively easy to measure Δa. A problem often encountered in relating Δa to δ is that Δa may not be uniform along the crack front.

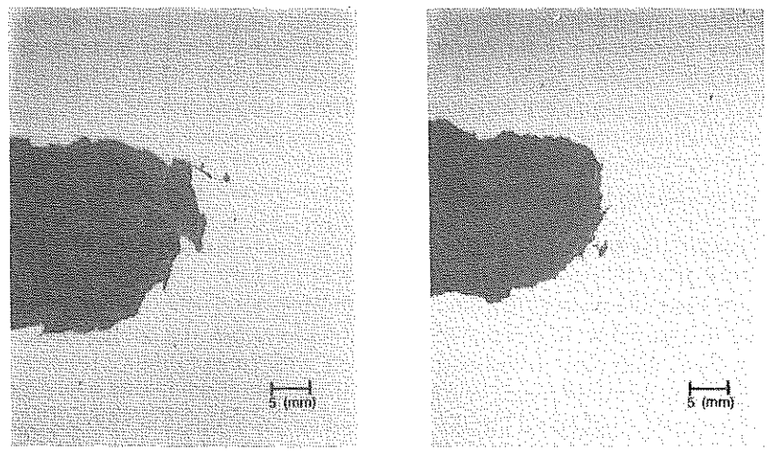

Fig 2 Fatigue precrack tip plus crack growth for specimen 15–3

Examples of the extent and location of crack growth (including SZW) for surface cracked specimens are provided in Reuter and Lloyd **(6)**. These results show that crack growth initiation occurs non-uniformly with no crack growth at the free surface.

Figure 3 shows typical results obtained from microtopography measurements. Note how smooth the crack tip region appears and that the region between the fatigue precrack and either cleavage or post-test fatigue is identified as fibrous fracture, but actually consists of SZW plus Δa. Therefore, to

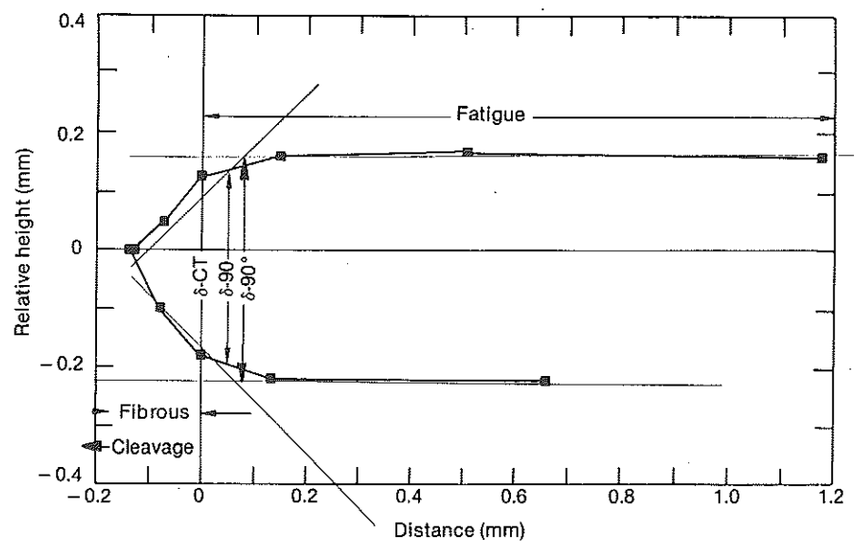

Fig 3 Schematic showing results obtained from microtopography

make direct comparisons between slicing and microtopography results, it is necessary to compare only Δa or SZW + Δa. One possible approach is to differentiate between SZW and fibrous crack growth while making topographic measurements. An alternative approach is to assume that SZW = $\delta/2$, and subtract this number from the microtopography results.

Crack-tip opening displacement, δ

δ is generally defined as the separation of the ends of the fatigue precrack; in this work that distance is designed δ-C(T). δ-C(T) was sometimes difficult to measure since the ends of the fatigue cracks were not easily located, see Fig. 2. It was not possible to simply state that δ-C(T) was the separation of the fatigue crack faces since it has been observed, with some of the C(T) specimens, that the ends of the precrack are located in the radius region of the crack tip. An alternative approach is to use Shih's definition (7) of δ as the intersection of a 90 degrees included angle with the actual crack front; this value was designated δ-90. This measurement was more easily obtained since it was no longer necessary to locate the ends of the fatigue precrack. But, sometimes it was not possible to measure δ-90 since CTOA decreased to less than 90 degrees or subcritical crack growth occurred and the 90 degrees included angle no longer intersected the crack front. Another definition of δ used, δ-90 degrees, is based on the intersection of a 90 degrees included angle with an extrapolated extension of the original crack planes. All three definitions of δ are shown schematically in Fig. 3. Figure 4 shows δ-90 and δ-90 degrees for a C(T) specimen. Observe that δ-90 degrees is essentially constant across the specimen, whereas this specimen showed a substantial variation in Δa. The δ-90 values in Fig. 4 are lower and show more variation than δ-90 degrees.

It is relatively easy to measure δ-C(T) with microtopography since the ends of the fatigue precracks can be located. Microtopographical measurements of

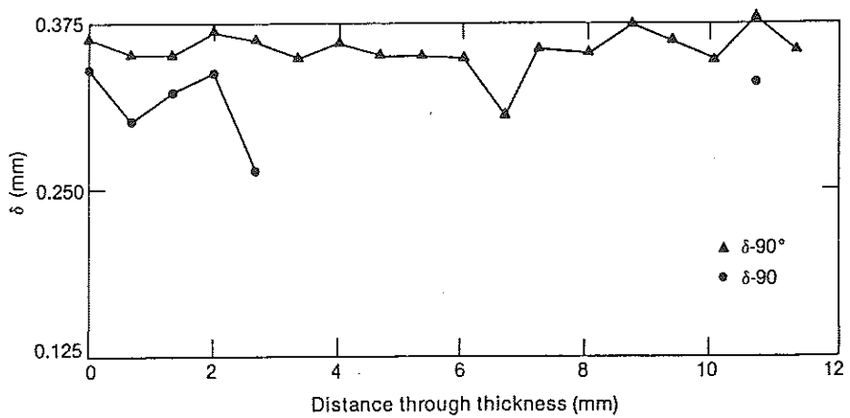

Fig 4 Comparison between δ-90 and δ-90 degrees for a C(T) specimen

the other two values of δ have the same success and difficulty identified for the slicing technique.

Discussion

This section summarizes and discusses data collected in the previous section and combines appropriate results into δ-Δa plots. These plots are extrapolated to $\Delta a = 0$ in order to estimate values of δ_{init} corresponding to initiation of crack growth. This section discusses constraint and identifies applicable values for the specimens used in this study.

Values of δ

δ_{init} is used in conjunction with numerical values of constraint to evaluate the efficacy of using data generated from C(T) and SE(B) specimens to predict crack initiation for structures containing surface flaws. When possible, measurements were made of δ-90, δ-90 degrees, and δ-C(T), but due to space limitations only δ-90 degrees is presented in the following figures. Because crack growth occurred in a non-uniform manner in the SC specimens, all data used in the figures are based on local values. Measurements at the surfaces were omitted if they were larger δ or smaller Δa than values from the interior. In those instances where $\Delta a > 0$ occurred, only those measurements were used to estimate Δa. Therefore, it is expected that values of δ_{init} obtained by extrapolating back to $\Delta a = 0$ will be low because this definition is for a micro-crack or local-crack growth initiation and not for macro-crack initiation.

Figure 5 shows a plot of δ versus Δa for the standard fracture toughness specimens. Note that crack initiation was estimated to occur at $\delta_{init} = 0.20$ mm. The value of δ is recorded in Table 1. The data plotted in Fig. 5 were obtained from both C(T) and SEN(B) specimens where $a/W = 0.61$ and $a/W = 0.57$, respectively. A statistical analysis of the C(T) and SEN(B) specimens showed that the regression correlation coefficient (R) was essentially unaffected (ranged from 0.86 to 0.88) by whether SEN(B) + C(T) or C(T) was analysed. In Fig. 5, Specimens 15-3, 13-3, and A82 had the smallest Δa. Data for the latter two specimens were obtained using microtopographic techniques that required that the SZW be subtracted from the measured value of Δa. This was done by assuming that SZW = $\delta/2$, which is reasonable since the CTOA is nominally 90 degrees. An accurate estimate of an upper limit value of δ_{init} may be obtained using Specimen 15-3. Figure 2 shows that local crack growth occurred for two slices in Specimen 15-3; therefore, δ_{init} is probably 0.20 mm (Fig. 5) but is less than 0.26 mm (Fig. 2). For Specimens A-82 and 13-3, only one of five measurements and two of six measurements, respectively, had $\Delta a > 0$. Therefore, the estimated value of $\delta_i = 0.20$ mm appears to be accurate.

Figure 6 is a plot of δ versus Δa for the CCP specimens. Note that these data do not vary as a function of the initial flaw size. The estimated value of δ_{init} is 0.13 mm, as recorded in Table 1. All the CCP specimens were examined

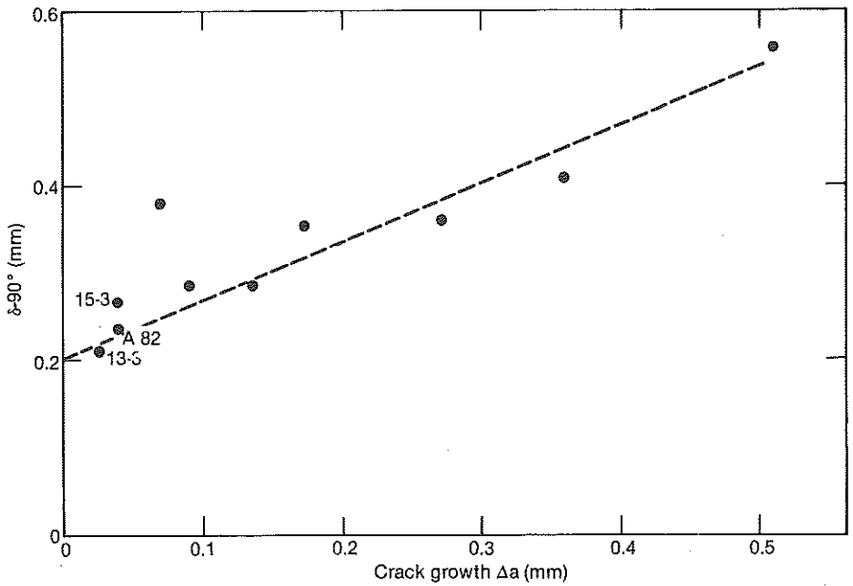

Fig 5 Plot of δ versus Δa for SEN(B) and C(T) specimens

by the slicing technique. The crack tip regions for Specimens 15 and 19 are shown in Figs 7 and 8, respectively. Figure 7 shows two different regions where crack growth has occurred. Figure 8 shows a crack front which suggests that crack growth has occurred. For Specimens 15 and 19, six of nine slices and

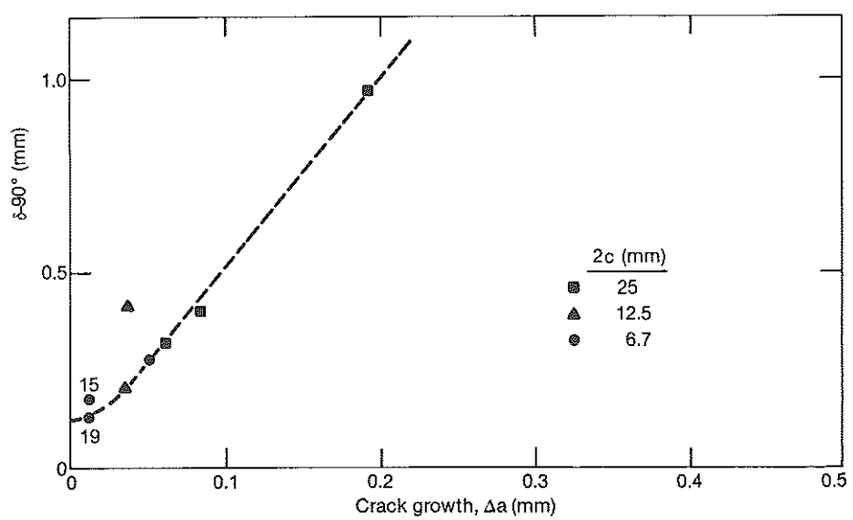

Fig 6 Plot of δ versus Δa for CCP specimens

Table 1 Measured δ and calculated constraint values for specified specimen configurations

Specimen configuration	δ_{init} *min**	δ_i *min*	*Constraint plain strain* σ'/σ^*†	‡
SEN(B)/C(T)	0.20–<0.26	0.27	2.89	2.53
CCP	0.13–0.17	0.69	1.90	1.41
SC	0.25–<0.30	0.375	2.07	—

* Underlined number is expected value, the other figure is estimated upper limit.
† Used σ, and assumed plane strain and no strain hardening to calculate σ_2 and σ_3.
‡ Calculated principal stresses with ABAQUS

nine of nine slices, respectively, had $\Delta a > 0$. Therefore, based on Figs 6 and 8, δ_{init} is probably 0.13 mm but could range up to 0.17 mm.

Figure 9 is a plot of δ versus Δa for SC specimens with $a/2c = 0.1$. This plot contains data obtained from $\theta = 45$ degrees and $\theta = 90$ degrees (maximum depth) where θ is measured from the free surface. For those specimens where Δa was measured by the microtopographic technique, the SZW was subtracted based on SZW $= \delta/2$. Since CTOA is nominally 60 degrees for the specimens where $\Delta a > 0.25$ mm, the use of SZW $= \delta/2$ results in a larger estimate of Δa than the actual, unknown, value. A decrease in Δa would result in a decrease in δ_{init}. Also, using data from sliced specimens ($\Delta a < 0.25$ mm) would result in a decrease in δ_{init}. The estimated value of δ_{init} using the solid line is 0.25 mm, and is recorded in Table 1. Figure 10 shows the crack tip region for Specimen E-1 where crack growth initiation has occurred. For this specimen, 14 of 20 slices had $\Delta a > 0$; therefore, δ_{init} is 0.25 mm based on Fig. 9, and is definitely less than 0.30 mm based on Fig. 10.

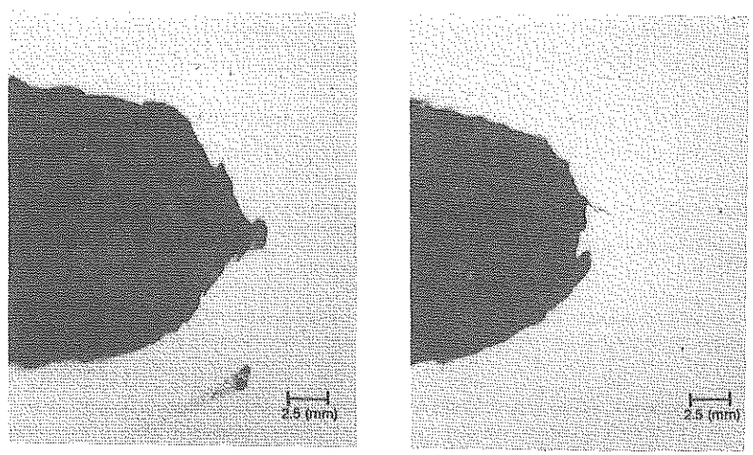

Fig 7 Fatigue precrack tip plus crack growth for CCP specimen 15

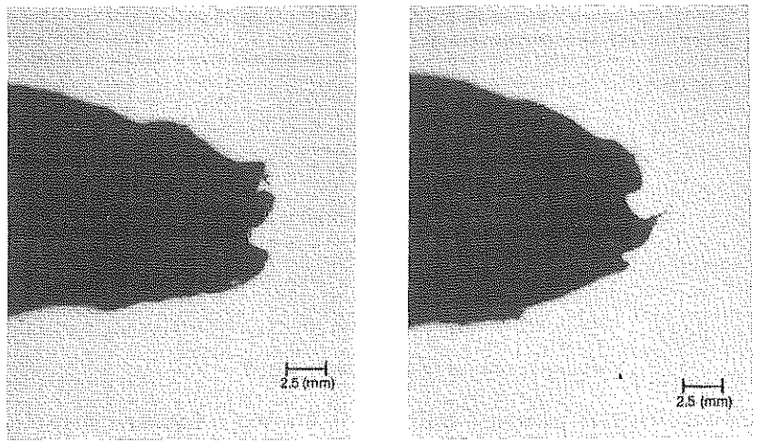

Fig 8 Fatigue precrack tip plus crack growth for CCP specimen 19

Constraint

Two terms were examined as possible candidates for the constraint parameter:

(1) $J = m\sigma_{ys}\delta$, where m is a measure of constraint.
Since the SC specimens, and possibly the CCP specimens, were no longer in a J-controlled field when crack growth initiation occurred, the values of J are questionable; therefore, m cannot be used as a measure of constraint for these specimens.

(2) Hydrostatic stress $= 1/3(\sigma_1 + \sigma_2 + \sigma_3) = \sigma'$, where σ_1, σ_2, and σ_3 are the principal stresses.

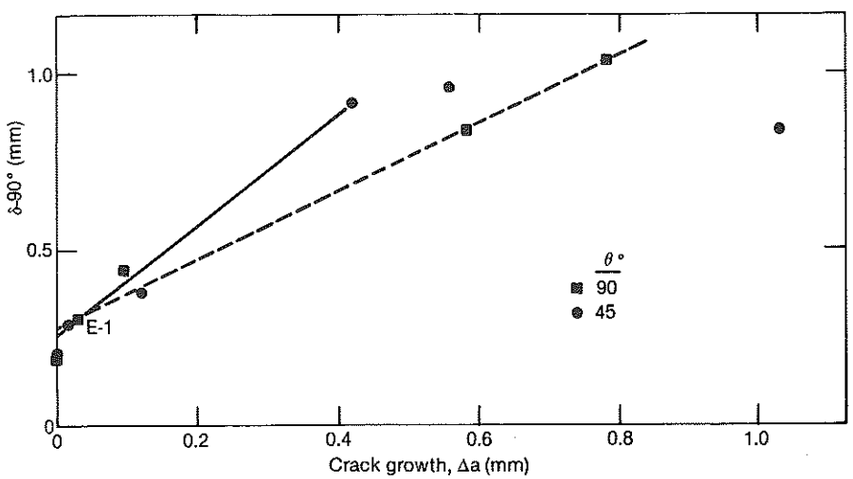

Fig 9 Plot of δ versus Δa for SC specimens

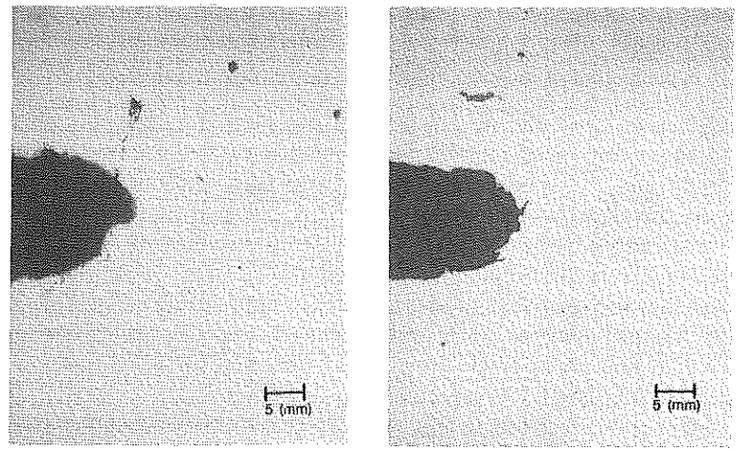

Fig 10 Fatigue precrack tip plus crack growth for SC Specimen E-1

This value (σ') was normalised by dividing by σ^*, the equivalent stress based on the von Mises yielding criterion. The values of σ_1, σ_2, and σ_3 were taken at the arbitrary location 2(δ-90) in front of the crack tip for all test specimens.

Elastic–plastic finite element analyses of both the CCP and SEN(B) specimens were conducted to calculate the principal stresses using the ABAQUS **(8)** structural mechanics computer program. Due to time restrictions, these analyses were limited to two dimensions assuming plane-strain conditions. The finite element solutions were based on the conventional linear strain-displacement relations assuming small geometry changes. In the crack tip region, eight-noded quadratic elements were collapsed to form six-noded triangular elements. Metal plasticity was accounted for using the experimentally obtained stress-strain data for A710 steel assuming isotropic hardening. Since only limited mesh resolution studies were conducted, the results must be considered approximate.

These principal stresses could then be used to calculate σ'/σ^*. Since the capabilities have not yet been developed at INEL for calculating the principal stresses for SC specimens, it was not possible to estimate σ'/σ^* in the same manner as used for the other two specimen configurations. Therefore, the following approach was used to calculate σ'/σ^* for the three configurations of concern.

(1) σ_1 was obtained with ABAQUS for SEN(B) and CCP specimens.
(2) σ_1 was calculated for SC specimens using methods developed by Wang **(9)** and Parks **(10)**.
(3) It was assumed that the material was elastic–perfectly plastic (no strain hardening) and that all specimens were under plane strain.

(4) $\sigma_3 = \sigma_1 - 1.15\sigma_{ys}$ and $\sigma_2 = (\sigma_1 + \sigma_3)/2$
were calculated.
(5) σ'/σ^* was calculated for each specimen configuration, see Table 1.

The values of σ'/σ^* and δ_{init} in Table 1 are plotted in Fig. 11, where the expected behaviour, increasing δ_{init} with decreasing σ'/σ^*, is observed between the SEN(B) and SC specimens, but no consistent relationship is observed among the three specimen configurations. It is expected that the relative constraint relationship, shown in Fig. 11, will continue even though σ'/σ^* will decrease if more accurate analytical procedures are used. There is very little likelihood that the relative δ_{init} positions are in appreciable error. This is supported by the facts that *no* crack growth was observed for an SC specimen at $\delta = 0.19$–0.20 mm while crack growth was observed for CCP Specimens 15 and 19 at $\delta = 0.17$ and 0.13, respectively.

The unexpected decrease in δ_{init} with decreasing constraint for the CCP specimen may be the result of competing processes at the crack tip. Early work of Lubahn **(11)** suggested that crack growth initiation will occur at either the tip of the precrack or interior of the specimen depending on constraint and its effect on fracture ductility. This variation of fracture location suggests an increase in δ with a decrease in σ'/σ^* similar to that observed for the SEN(B) and SC specimens. But it does not predict the behaviour of the CCP specimens. However, at low constraint a different type of initiation could be occurring that is similar to the shear process observed in single crystals. The shearing action causes the material to simply slide and does not cause a crack to form, but could cause a perturbation in the crack tip radius that is defined

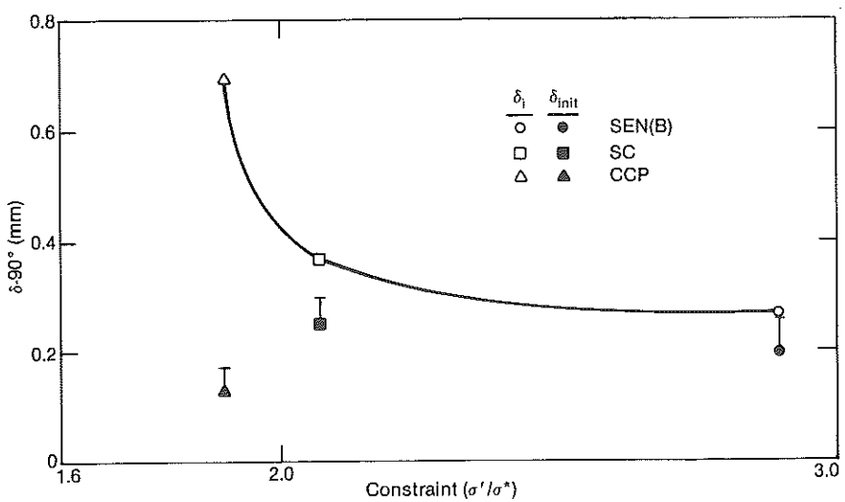

Fig 11 Plot of δ_{init} and δ_i versus constraint σ'/σ^*

as crack initiation in this study. As the constraint decreases, this type of slip behaviour is fostered, thereby causing a decrease in δ_{init} with decreasing σ'/σ^*. At constraint levels corresponding to the CCP specimen, slip, instead of cracking, may be dominating the crack tip process causing the decrease in δ_{init}.

A second evaluation was conducted based on using δ at some distance from initiation of crack growth. This was done to remove some of the statistical variations associated with crack initiation and to reduce effects of different mechanisms of crack growth initiation, if they occur. This was done by using δ_i associated with $\Delta a = 0.2$ mm using

δ_i at Δa where $\Delta a = \Delta a$ at $\delta_{init} - \frac{1}{2}\delta + 0.2$ mm.

These results are shown in Fig. 11; δ_i shows consistent behaviour with σ'/σ^*.

Summary and conclusions

Different types of data are obtained with the slicing and microtopography techniques. The sliced specimens will frequently show the 'real' crack growth that occurred at the crack tip, whereas the microtopographic technique provides SZW plus Δa. SZW can be estimated from δ and then subtracted from the fibrous fracture length to obtain a useful estimate of Δa; however, the accuracy of assuming SZW $= \frac{1}{2}\delta$ has not been verified by test results. It has been shown that δ-90 degrees may provide useful data for characterizing crack initiation. Values of δ_{init} (δ at Δa just greater than zero) and δ_i (δ at $\Delta a = 0.2$ mm) were measured for each of the three significant specimen configurations.

This work has shown that the use of δ_i, which corresponds to $\Delta a = 0.20$ mm, to predict crack initiation (δ_{init}) of specimens containing surface cracks may be acceptable. But this apparent agreement appears to be fortuitous.

It was found that δ_{init} did not vary in a consistent manner with constraint, σ'/σ^*. This shows that it would be very difficult to predict crack growth initiation for a structure based on data obtained from standard fracture toughness specimens. (It is necessary to conduct additional work to define statistical variations in crack growth initiation and to identify mechanisms of crack growth initiation.)

It was found that δ_i varied in a consistent manner with constraint. This suggests that it will be possible to predict crack growth initiation associated with Δa (including SZW) of 0.20 mm for a structure based on data obtained from standard fracture toughness specimens. Since $\Delta a = 0.2$ mm is an arbitrary amount of crack growth, regardless of specimen size, for measuring δ_i some error will be introduced into the comparison. It is necessary that three-dimensional finite element techniques be used to calculate more accurate values of σ'/σ^* to provide an accurate relationship between δ and σ'/σ^*.

These latter two conclusions are sensitive to the δ-Δa curves and the location of crack initiation versus location where σ'/σ^* is calculated.

Acknowledgements

This work was supported by the U.S. Department of Energy Office of Energy Research, Office of Basic Energy Sciences, under DOE Contract No. De-AC07-76ID01570. The authors acknowledge the help of Professor D. M. Parks of MIT, Professor G. Irwin of the University of Maryland, G. L. Fletcher, and D. A. Cullen for her patience in typing the manuscript.

References

(1) Standard test method for crack-tip opening displacement (CTOD) fracture toughness measurement, E1290-89, *ASTM Standards*, (1989) Section **3**, pp. 913–928.
(2) MATSOUKAS, G., COTTERELL, B., and MAI, Y.-W. (1986) Hydrostatic stress and crack opening displacement in three-point bend specimens with shallow cracks, *J. Mech. Phys. Solids*, **34**, 455–510.
(3) Standard test method for J_{Ic}, a measure of fracture toughness, E813-87, *ASTM Standards*, (1988) pp. 686–700.
(4) KOBAYASHI, T., IRWIN, G. R., and ZHANG, X. J. (1989) Topographic examination of fracture surfaces in fibrous-cleavage transition behavior, *ASTM STP 827*, pp. 234–251, ASTM Philadelphia.
(5) ZHANG, X. J., ARMSTRONG, R. W., and IRWIN, G. R. (1986) Cleavage fracturing stages at microsize inclusions in pressure vessel steel weldmetal, *J. Materials Science Letters*, **5**, 961–964.
(6) REUTER, W. G. and LLOYD, W. R. (1990) Measurements of CTOD and CTOA around surface-crack perimeters and relationships between elastic and elastic–plastic CTOD values, *ASTM STP 1060*, ASTM Philadelphia.
(7) SHIH, C. F. (1981) Relationships between the *J*-integral and the crack opening displacement for stationary and extending cracks, *J. Mechanics and Physics of Solids*, **29**, 305–326.
(8) *ABAQUS*, Hibbit, Karlsson, and Sorenson, Inc., Providence, RI.
(9) WANG, Y. (1988) Analysis of fracture initiation in surface cracked plate, M.S. Thesis, Dept. of Mech. Engng, Massachusetts Institute of Technology.
(10) PARKS, D. M. (1990) A surface crack review: elastic and elastic–plastic behavior, *ASTM STP 1060*, ASTM Philadelphia.
(11) LUBAHN, J. D. (1956) Effect of temperature on the fracture behavior of mild steel, *Welding Research Supplement*, November 1956, pp. 557-s–568-s.